COMMUNICATION

Toward Efficient Orange Emissive Carbon Nanodots through Conjugated sp^2-Domain Controlling and Surface Charges Engineering

Songnan Qu, Ding Zhou, Di Li, Wenyu Ji, Pengtao Jing, Dong Han, Lei Liu, Haibo Zeng, and Dezhen Shen**

Luminescent carbon nanodots (CNDs) have attracted great interest because they for the first time endow carbon nanomaterials with excellent luminescent property and open a promising prospect of C-luminescence.[1–3] The first reported CNDs exhibited very weak luminescence.[4] In the last decade, photoluminescent (PL) quantum yields of CNDs have been greatly improved through various chemical methods, such as heteroatom doping, surface passivation or surface engineering. Strong blue luminescent CNDs with PL quantum yields higher than 80%,[5] and green luminescent CNDs with PL quantum yields higher than 50%[6] were achieved. In addition, a lot of works revealed that CNDs have distinct benefits, such as chemical stability, dispersibility in water, low photobleaching, biocompatibility, and low toxicity, making them the new-generation luminescent materials, superior to conventionally used both fluorescent organic dyes and luminescent inorganic quantum dots (QDs).[7,8] Owing to these merits, CNDs can be used in a wide range of technologies, such as bioimaging,[9,10] fluorescent probes,[11,12] optoelectronic devices,[13–17] and white light emitting diodes (WLEDs).[18–21] However, efficient long-wavelength (orange and red light regions) emissive CNDs are very scarce due to lack of effective synthesized method and blur luminescence mechanism, which greatly hinder their development and applications. The bandgap transitions of CNDs are from conjugated sp^2-domains. Theoretical calculations demonstrated that the bandgap of CNDs can be tuned by modulating the size of conjugated sp^2-domains.[22] In this aspect, CNDs are also called carbon quantum dots. It should be noted that the size of sp^2-domains is the real domination of quantum confinement effect, not the particle size. It is suggested that increasing particle sizes to achieve increased conjugated sp^2-domain is favorable for orange and red emissions, but large sized particles usually contain large surface areas and increased surface defects, leading to non-efficient emissions. Pang and co-workers developed a controllable wet oxidation method for synthesizing red emissive CNDs (centered at 608 nm, PL quantum yield of 1.8%) through surface oxidation of larger sized CNDs.[23] The main absorption band of the CNDs is in UV region. Their red emission is supposed from the surface states created by surface oxidation. Lin and co-workers reported efficient red emissive CNDs (centered at 603 nm, PL quantum yield of 26.1%) prepared from p-phenylenediamine through solvothermal method.[24] Ding et al. reported efficient red emissive CNDs (centered at 625 nm, PL quantum yield of 24%) prepared from p-phenylenediamine and urea through hydrothermal method via column chromatography.[25] The main absorption band of the CNDs can cover blue and green wavelength regions, indicating large conjugated sp^2-domain. The mechanism for the high efficient red emission from the CNDs is unclear. The authors pointed that large particle sizes and high nitrogen contents are responsible for the efficient red emission. Thus, it is of urgent need to develop an effective method and theory to prepare orange or red emissive CNDs with high PL quantum yields.

Recently, CND-based phosphors, as new generation of environmental friendly phosphors, have been paid increasing attentions for lighting and display applications. A few efficient blue and green emissive CND-based phosphors have been reported by several groups for application in WLEDs.[18–21] For indoor lighting, warm WLEDs with correlated color temperature (CCT) lower than 4000 K are strongly desired.[26,27] However, it is hard to realize warm WLEDs only based on CNDs due to lack of efficient orange or red luminescent CND-based phosphors. In our previous work, we reported an effective method of preparing green emissive CNDs through one-step microwave synthesis from citric acid and urea.[28,29] In this work, we report new orange emissive CNDs and propose a new strategy of realizing efficient orange emission from the CNDs through conjugated sp^2-domain controlling and surface charges engineering. CNDs with large conjugated sp^2-domain can be prepared via a solvothermal route from citric acid and urea using dimethylformamide (DMF) as solvent, which is the basis of bandgap orange emission. Highly orange emissive CNDs (CND1) with PL quantum yield of 46% were achieved through surface metal-cation-functionalizing from the solvothermally synthesized

Prof. S. Qu, Dr. D. Zhou, Dr. D. Li, Dr. W. Ji, Dr. P. Jing, Dr. D. Han, Prof. L. Liu, Prof. D. Shen
State Key Laboratory of Luminescence and Applications
Changchun Institute of Optics
Fine Mechanics and Physics
Chinese Academy of Sciences
3888 Eastern South Lake Road, Changchun, Jilin 130033, China
E-mail: qusn@ciomp.ac.cn; shendz@ciomp.ac.cn
Prof. H. Zeng
Institute of Optoelectronics & Nanomaterials
College of Material Science and Engineering
Nanjing University of Science and Technology
Nanjing 210094, China

DOI: 10.1002/adma.201504891

CNDs. Our results demonstrated that surface charges engineering by surface metal-cation-functionalization could decrease overlap between absorption and emission, leading to small self-absorption, which is a benefit for efficient orange emission. To the best of our knowledge, it is the highest PL quantum yield of CNDs in orange light region. Using CND1, we further prepared efficient orange emissive starch/CND1 phosphors (PL quantum yield of 21%) and realized warm WLEDs (Commission Internationale d'Éclairage (CIE) coordinates (0.41, 0.45), CCT: 3708 K) by using green and orange emissive starch/CND phosphors.

The metal-cation-functionalized CNDs were prepared by treating solvothermally synthesized CNDs with an alkali. In detail, citric acid (1 g) and urea (2 g) were reacted at 160 °C for 6 h under solvothermal condition in 10 mL DMF and then cooled to room temperature. The obtained dark brown solution was mixed with 20 mL alkali (NaOH or KOH) aqueous solution (50 mg mL^{-1}), stirred for 1 min, and then centrifuged at 16000 r min^{-1} for 10 min. The precipitate was collected, dissolved in water and centrifuged (16 000 r min^{-1}, 10 min) twice to wash off residual salts and alkali, and then freeze-dried to give the dark products of CND1. To understand the effect of the surface metal-cation-functionalization, non-metal-cation-functionalized CNDs (CND2) were also prepared. 100 mg CND1 were further dissolved in 20 mL dilute HCl aqueous solution (5 wt%) and stirred for 10 min to take off the surface passivated metal cations. The solution was centrifuged at 16000 r min^{-1} for 10 min. The precipitate was collected, dissolved in water and centrifuged (16000 r min^{-1}, 10 min) twice to wash off residual salts and HCl, and then freeze-dried to give the dark products of non-metal-cation-functionalized CNDs (CND2).

The morphologies of the CND1 and CND2 were characterized using transmission electron microscopy (TEM) and atomic force microscopy (AFM). TEM image of CND1 shows their diameters in the range from 4 to 10 nm (**Figure 1**b and Figure S4a, Supporting Information). The high-resolution TEM (HRTEM) image shows the circular shape of the CND1, with visible crystalline lattice fringes (Figure 1c). The interlayer spacing of 0.21 nm corresponds to the d-spacing of the graphene {1-100} planes.[30] Carefully observing, most of the CND1 exhibit uniform atomic arrangements, indicating high degree of crystallinity. The AFM image of CND1 reveals their topographic heights in the range 0.6 to 2.5 nm (Figure 1a and Figure S4b, Supporting Information), indicating that the CND1 primarily consisted of two to eight layers of graphene-like sheets. Similar results can be observed in CND2 (Figure S1, Supporting Information), indicating the same multilayer graphene-like

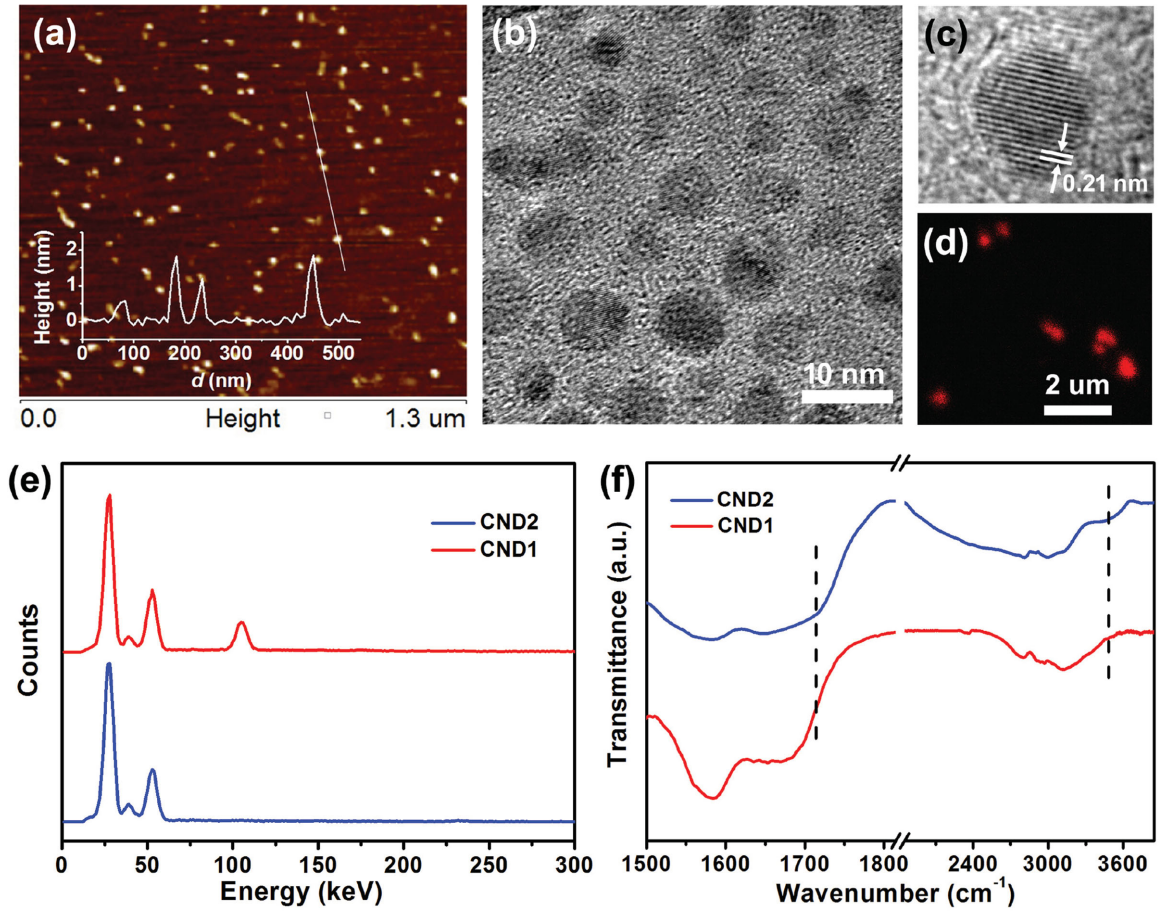

Figure 1. a) AFM, b) TEM, and c) HRTEM images of CND1. d) Confocal microscopy image of CND1 deposited from ethanol solution onto a glass substrate under 488 nm excitation. e) EDX and f) FT-IR spectra of CND1 and CND2.

Table 1. Atomic ratios of C, N, O, Na in EDX results of CND1 and CND2.

	C	N	O	Na
CND1	3.42	1	1.04	0.31
CND2	3.32	1	0.93	0

core structures. Confocal microscopy image of CND1 on glass substrate deposited from dilute ethanol solution exhibits dispersively bright luminescent dots under 488 nm excitation, indicating luminescent property of each CND (Figure 1d).

The chemical compositions of CND1 and CND2 were investigated by energy dispersive X-ray spectrometer (EDX). EDX spectrum of CND1 shows four peaks at 0.27, 0.39, 0.53, and 1.05 keV (Figure 1e), corresponding to C, N, O, and Na, respectively. The atomic ratios of C, N, O in EDX results of CND1 and CND2 are similar, while no Na signal was observed in EDX spectrum of CND2 (**Table 1**). C/N atomic ratio in EDX results is about 3:1, indicating CND1 and CND2 are nitrogen-rich CNDs. It should be noted that C/O atomic ratio of citric acid and urea is about 1:1, which is much lower than that of CND1 and CND2 (about 3:1), suggesting that a large portion of oxygen atoms was lost during the solvothermal treatment. It can be concluded that CND1 and CND2 have similar C, N, O contents, while metal cations were taken off in CND2. The surface functional groups of CND1 and CND2 were further detected by Fourier transform infrared (FT-IR) spectrometer (Figure 1f). In FT-IR spectra, broad absorption bands at 3050–3650 cm^{-1} are assigned to ν(O—H) and ν(N—H). Very broad band absorbing at 1850–3000 cm^{-1} is only observed in CND2, which is attributed to —OH groups in strong hydrogen bonding.[31] Absorption band peaked at 1710 cm^{-1} is observed in CND2, which is assigned to ν(C=O) in carboxyl groups. In FT-IR spectrum of CND1, the absorption bands at 3430–3650 cm^{-1} (ν(O—H)) and absorption band peaked at 1710 cm^{-1} (ν(C=O)) are greatly decreased. The very broad band absorbing at 1850–3000 cm^{-1} is non-observed in CND1. In contrast, strong absorption band peaked at 1580 cm^{-1} is observed in CND1, which is assigned to ν_{as}(COO) in carboxylate groups.[31] The FT-IR results demonstrate abundant carboxylate groups functionalized on the surfaces of CND1, which changed to carboxyl groups on CND2. Zeta potential measurements were carried out to detect the surface potential of CND1 and CND2. The zeta potentials of CND1 and CND2 in aqueous solution are –35.7 and –17.3 mV, respectively. The more negative surface potential of CND1 in aqueous solution could be due to the surface-contained more negative ionized carboxylate radicals, which changed to less negative carboxyl groups, leading to less negative surface potential of CND2.

Based on the chemical structures of the starting materials and experimental results, a possible growth mechanism for the CND1 and CND2 is illustrated in **Scheme 1**. Urea and citric acid could assemble into a nanoplate structure through the inter-molecular H-bonding. Under solvothermal condition, dehydrolysis process happened between urea and citric acid to form nitrogen-rich CNDs with abundant carboxyl, hydroxyl, and amide groups on the surface. Upon adding alkali (NaOH or KOH) solution, carboxyl and phenolic hydroxyl groups are neutralized to give CND1. The surface functionalized metal cations can be further taken off in dilute HCl aqueous solution to give CND2.

It is interesting to find that CND1 exhibits strong orange luminescence with less excitation-wavelength-dependent PL in dilute ethanol solution (**Figure 2**a). The strongest emission of

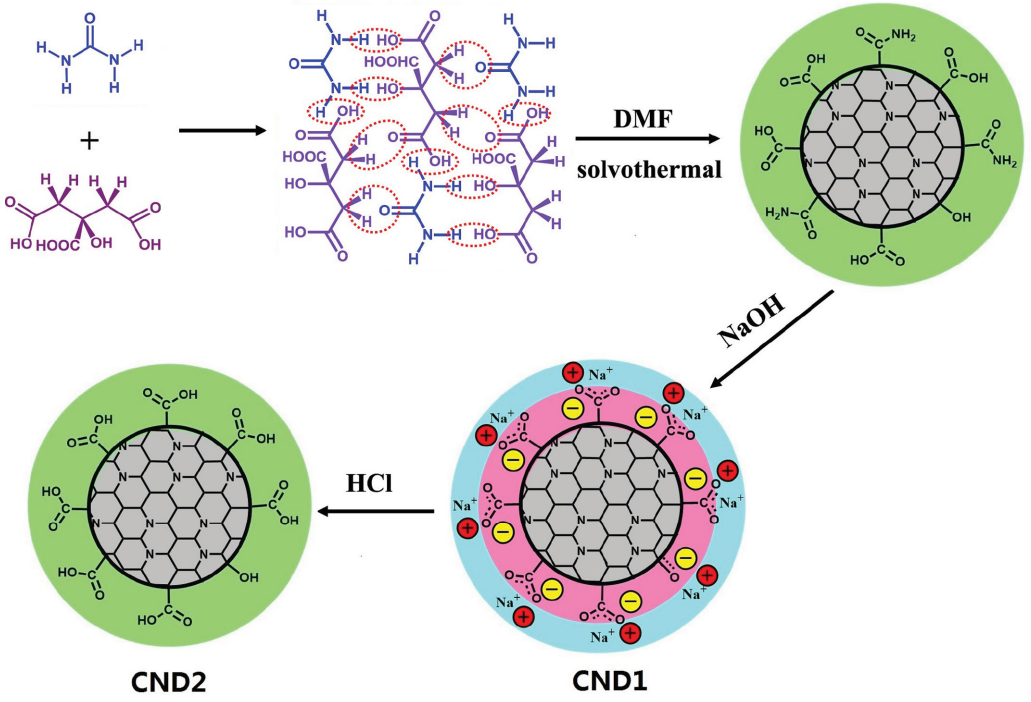

Scheme 1. A possible growth mechanism for CND1 and CND2.

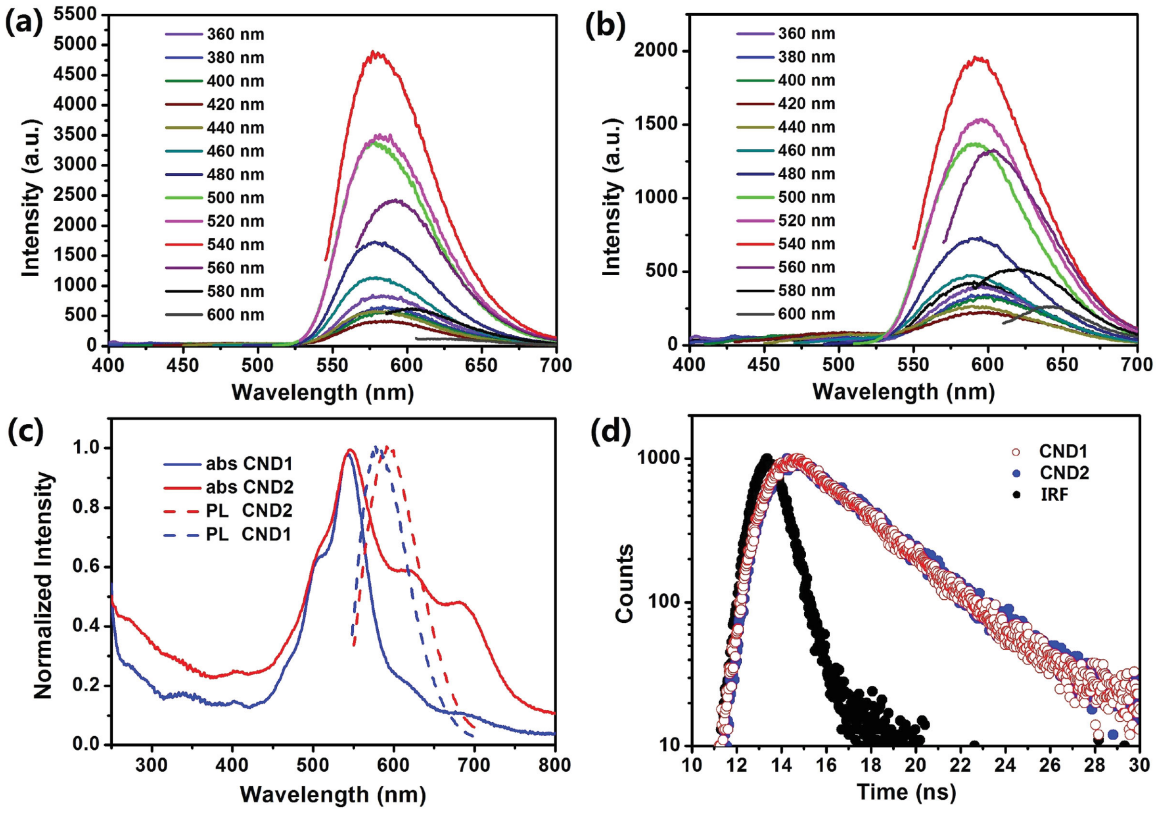

Figure 2. PL spectra of a) CND1 and b) CND2 at different excitation wavelengths. d) UV–vis absorption spectra and PL spectra (540 nm excitation) of CND1 and CND2 dilute ethanol solution. c) Time resolved luminescence decay curves collected at 580 nm for CND1 and CND2 (540 nm excitation) (IRF = instrument response function).

CND1 dilute ethanol solution was observed centered at 580 nm under 540 nm excitation, with a PL quantum yield of 46%. In contrast, CND2 exhibits red-shifted weak orange luminescence (Figure 2b). The strongest emission of CND2 dilute ethanol solution was observed at 590 nm, with a PL quantum yield of 6% under 540 nm excitation. The UV–vis spectrum of CND1 display obvious visible absorption band peaked at 540 nm (Figure 2c), indicating large sized conjugated sp^2-domain in the particles. CND2 also display obvious visible absorption band (peaked at 540 nm), but the long wavelength shoulder of the visible absorption band is much broader than that of CND1, leading to larger overlap between absorption and emission. The PL decays of the orange emissions from CND1 and CND2 in ethanol solution are mono-exponential with similar lifetime of 3.8 ns (Figure 2d), indicating the similar luminescent process. It can be concluded that the much higher PL quantum yield of CND1 is due to smaller self-absorption because of smaller overlap between absorption and emission, on comparing with CND2. The obvious visible absorption band (peaked at 540 nm), less excitation-wavelength-dependent and surface-independent orange emissive process indicates that the orange emission of CND1 and CND2 are bandgap emission from the conjugated sp^2-domain in the nitrogen-rich multilayer graphene-like cores. The optical properties of the hydrothermal and microwave synthesized CNDs from the citric acid (1 g) and urea (2 g) were also analyzed for comparison. The hydrothermally synthesized CNDs showed intense blue emission (λ_{em} = 443 nm) with a main absorption band in UV region centered at 340 nm (Figure S2, Supporting Information), which is similar to literature.[32] The microwave synthesized CNDs showed intense green emission (λ_{em} = 526 nm) with a main absorption band in UV region centered at 420 nm.[29] It can be seen that DMF in the solvothermal synthetic route is a good solvent for the formation of CNDs with large sized conjugated sp^2-domain, which is the basis of bandgap orange emission.

Based on the results above, we propose that the long wavelength shoulders of the visible absorption band of CND1 and CND2 are due to electron transitions from surface states, which could absorb some part of the orange emissions from the multilayered graphene-like cores, and are against efficient orange emission. A possible mechanism for the enhanced orange emission is illustrated in **Scheme 2**. Surface metal-cation-functionalization could cause increased carboxylate ions on the inner surface of CND1, leading to electron-rich property of the inner surface, as demonstrated by zeta potential results. The rich electrons could occupy the energy levels of the surface states and lift the Fermi level of the CNDs. Thus, orange-light-induced electron transitions from the surface states are non-favorite, leading to smaller self-absorption and enhancing the output orange emission of CND1.

The luminescence of CND1 and CND2 are greatly quenched in the solid aggregate states. In our previous work, we reported a universal technique for preparing efficient

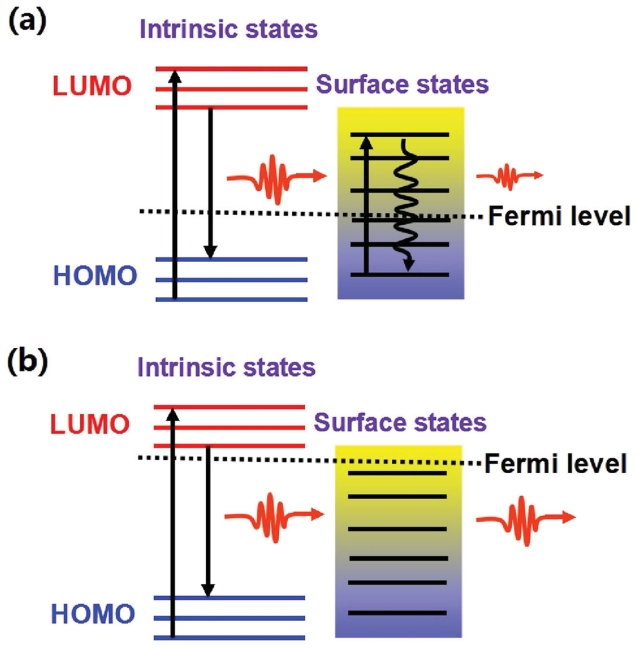

Scheme 2. Possible energy structures and output orange emission processes in a) CND2 and (b) CND1.

CND-based phosphors through effective dispersion of CNDs by integrating CNDs with starch particles.[20] Efficient green emissive starch/CND phosphors and the phosphor-based WLEDs with CIE (0.26, 0.33) were prepared. Due to the strong orange luminescence of CND1, orange emissive starch/CND1 phosphors were prepared and employed as the color conversion layer to fabricate a warm WLED prototype. **Figure 3**a shows the fluorescence images of the starch/CND1 phosphors. The starch/CND1 phosphors with particle size distribution ranging from 10 to 30 μm possess a PL quantum yield of 23% under 540 nm excitation (Figure 3a). To realize warm white-light LEDs, the mixture of orange emissive starch/CND1 phosphors and epoxy silicone resin are deposited onto a cool white-light LED fabricated by applying our previously reported green emissive starch/CND phosphors.[20] A warm WLED only based on starch/CND phosphors is obtained (Figure 3b), and its CIE and CCT are (0.41, 0.45) and 3708 K, respectively (Figure 3d,f). In the emission spectrum, the wide emissions ranging from 550 to 650 nm are brought by orange emissive starch/CND1 phosphors (Figure 3e). It can be concluded that the orange emissive starch/CND phosphors are promising candidates for practical lighting applications.

In conclusion, we developed new solvothermally synthesized orange emissive CNDs and proposed a new strategy of realizing

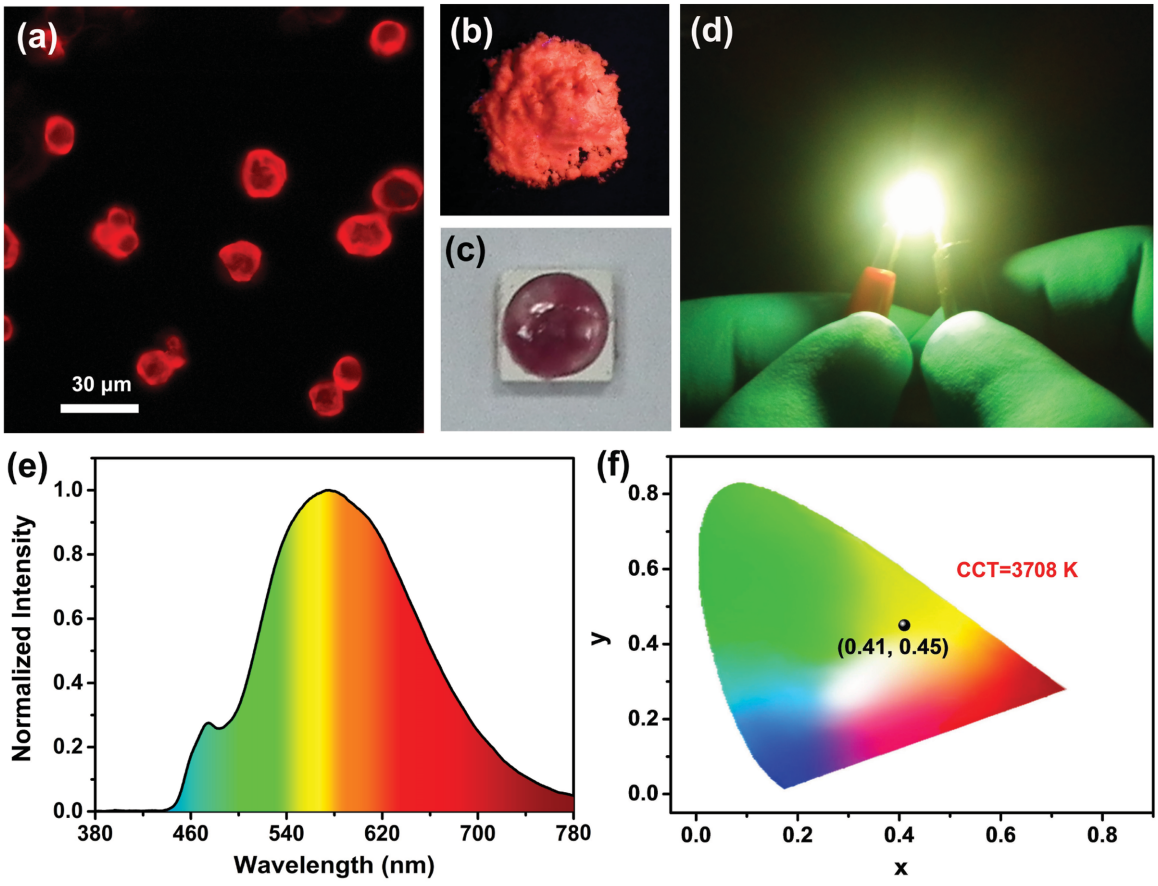

Figure 3. Fluorescence image of the starch/CND1 phosphors under a) fluorescence microscope (green light excitation) and b) a UV lamp. c) The photograph of WLED, which is fabricated by integrating starch/CND1 phosphors and green starch/CND-based LED, is taken at sunlight. d) The photograph of the working WLED with warm white emission. e) The corresponding emission spectrum and f) the color coordinate of the WLED.

efficient orange emission from the CNDs through conjugated sp^2-domain controlling and surface charges engineering. We demonstrated that DMF in the solvothermal synthetic route is a good solvent for the formation of CNDs with large sized conjugated sp^2-domain, which is the basis of orange bandgap emission. Enhanced orange emissive CND1 with PL quantum yield of 46% was realized through surface charges engineering by surface metal-cation-functionalization. Their orange emissions were greatly decreased after taking off the surface functionalized metal ions. These results revealed that surface charges engineering by surface metal-cation-functionalization could decrease overlap between absorption and emission, and thus benefit efficient output emissions. A possible mechanism was proposed that surface metal-cation-functionalization could lift the Fermi level of the CNDs, leading to smaller self-absorption and enhancing the output orange emission. Using CND1, we further prepared efficient orange emissive starch/CND1 phosphors (PL quantum yield of 21%) and realized warm WLEDs (CIE: (0.41, 0.45), CCT: 3708 K) by only using the green and orange emissive starch/CND phosphors. We prospect the proposed strategy will promote the development and application of CNDs.

Experimental Section

Characterizations: TEM observations were performed on a FEI Tecnai-G2-F20 TEM at 200 kV. AFM measurements were performed on a SA400HV with a Seiko SPI3800N controller. EDX analysis was performed by a EDAX Genesis 2000 Energy Dispersive Spectroscopy. FT-IR spectra were performed with a Perkin–Elmer spectrometer (Spectrum One B). Zeta potential measurement was performed using a Zetasizer Nano-ZS (Malvern Instruments). The confocal microscopy image was performed with C2+ confocal microscope system (Nikon confocal instruments). PL spectra were collected using a Hitachi F-7000 spectrophotometer and UV–visible absorption spectra were recorded on a Shimadzu UV-3101PC spectrophotometer. Photoluminescence quantum yields were obtained in a calibrated integrating sphere in FLS920 spectrometer. Fluorescence lifetimes were measured using FLS920 time-corrected single photon counting system.

Supporting Information

Supporting Information is available from the Wiley Online Library or from the author.

Acknowledgements

This work was supported by the National Natural Science Foundation of China (Grant Nos. 61274126, 61306081, and 51572128), Outstanding Young Scientists Program of Chinese Academy of Sciences, Jilin Province Science and Technology (Research Project Nos. 20140101060JC, 20150519003JH, and 20130522142JH).

Received: October 5, 2015
Revised: January 2, 2016
Published online: February 26, 2016

[1] X. Li, M. Rui, J. Song, Z. Shen, H. Zeng, *Adv. Funct. Mater.* **2015**, *25*, 4929.
[2] X. T. Zheng, A. Ananthanarayanan, K. Q. Luo, P. Chen, *Small* **2015**, *11*, 1620.
[3] S. Y. Lim, W. Shen, Z. Gao, *Chem. Soc. Rev.* **2015**, *44*, 362.
[4] X. Xu, R. Ray, Y. Gu, H. J. Ploehn, L. Gearheart, K. Raker, W. A. Scrivens, *J. Am. Chem. Soc.* **2004**, *126*, 12736.
[5] Z. Xie, F. Wang, C. Liu, *Adv. Mater.* **2012**, *24*, 1716.
[6] X. Wang, L. Cao, S. T. Yang, F. Lu, M. J. Meziani, L. Tian, K. W. Sun, M. A. Bloodgood, Y.-P. Sun, *Angew. Chem. Int. Ed.* **2010**, *49*, 5310.
[7] S. N. Baker, G. A. Baker, *Angew. Chem. Int. Ed.* **2010**, *49*, 6726.
[8] J. C. G. Esteves da Silva, H. M. R. Goncalves, *TrAC Trends Anal. Chem.* **2011**, *30*, 1327.
[9] Y.-P. Sun, B. Zhou, Y. Lin, W. Wang, K. A. S. Fernando, P. Pathak, M. J. Meziani, B. A. Harruff, X. Wang, H. Wang, P. G. Luo, H. Yang, M. E. Kose, B. Chen, L. M. Veca, S.-Y. Xie, *J. Am. Chem. Soc.* **2006**, *128*, 7756.
[10] D. Qu, M. Zheng, J. Li, Z. Xie, Z. Sun, *Light: Sci. Appl.* **2015**, *4*, e364.
[11] A. Zhu, Q. Qu, X. Shao, B. Kong, Y. Tian, *Angew. Chem. Int. Ed.* **2012**, *51*, 7185.
[12] S. Qu, H. Chen, X. Zheng, J. Cao, X. Liu, *Nanoscale* **2013**, *5*, 5514.
[13] F. Wang, Y. Chen, C. Liu, D. Ma, *Chem. Commun.* **2011**, *47*, 3502.
[14] X. Zhang, Y. Zhang, Y. Wang, S. Kalytchuk, S. V. Kershaw, Y. Wang, P. Wang, T. Zhang, Y. Zhao, H. Zhang, T. Cui, Y. Wang, J. Zhao, W. W. Yu, A. L. Rogach, *ACS Nano* **2013**, *7*, 11234.
[15] S. H. Song, M.-H. Jang, J. Chung, S. H. Jin, B. H. Kim, S.-H. Hur, S. Yoo, Y.-H. Cho, S. Jeon, *Adv. Opt. Mater.* **2014**, *2*, 1016.
[16] J. Tang, Y. Zhang, B. Kong, Y. Wang, P. Da, J. Li, A. A. Elzatahry, D. Zhao, X. Gong, G. Zheng, *Nano Lett.* **2014**, *14*, 2702.
[17] D.-Y. Guo, C.-X. Shan, S.-N. Qu, D.-Z. Shen, *Sci. Rep.* **2014**, *4*, 7469.
[18] X. Guo, C.-F. Wang, Z.-Y. Yu, L. Chen, S. Chen, *Chem. Commun.* **2012**, *48*, 2692.
[19] C. Sun, Y. Zhang, K. Sun, C. Reckmeier, T. Zhang, X. Zhang, J. Zhao, C. Wu, W. W. Yu, A. L. Rogach, *Nanoscale* **2015**, *7*, 12045.
[20] M. Sun, S. Qu, Z. Hao, W. Ji, P. Jing, H. Zhang, L. Zhang, J. Zhao, D. Shen, *Nanoscale* **2014**, *6*, 13076.
[21] Y. Wang, S. Kalytchuk, L. Wang, O. Zhovtiuk, K. Cepe, R. Zboril, A. L. Rogach, *Chem. Commun.* **2015**, *51*, 2950.
[22] M. A. Sk, A. Ananthanarayanan, L. Huang, K. H. Lim, P. Chen, *J. Mater. Chem. C* **2014**, *2*, 6954.
[23] L. Bao, C. Liu, Z.-L. Zhang, D.-W. Pang, *Adv. Mater.* **2015**, *27*, 1663.
[24] K. Jiang, S. Sun, L. Zhang, Y. Lu, A. Wu, C. Cai, H. Lin, *Angew. Chem. Int. Ed.* **2015**, *54*, 5360.
[25] H. Ding, S.-B. Yu, J.-S. Wei, H.-M. Xiong, *ACS Nano* **2016**, *10*, 484.
[26] M. R. Krames, O. B. Shchekin, R. Mueller-Mach, G. O. Mueller, L. Zhou, G. Harbers, M. G. Craford, *J. Disp. Technol.* **2007**, *3*, 160.
[27] X. Li, J. D. Budai, F. Liu, J. Y. Howe, J. Zhang, X.-J. Wang, Z. Gu, C. Sun, R. S. Meltzer, Z. Pan, *Light: Sci. Appl.* **2013**, *2*, e50.
[28] S. Qu, X. Wang, Q. Lu, X. Liu, L. Wang, *Angew. Chem. Int. Ed.* **2012**, *51*, 12215.
[29] S. Qu, X. Liu, X. Guo, M. Chu, L. Zhang, D. Shen, *Adv. Funct. Mater.* **2014**, *24*, 2689.
[30] T.-F. Yeh, C.-Y. Teng, S.-J. Chen, H. Teng, *Adv. Mater.* **2014**, *26*, 3297.
[31] P. Barczy ski, I. Kowalczyk, M. Grundwald-Wyspia ska, M. Szafran, *J. Mol. Struct.* **1999**, *484*, 117.
[32] X. Li, S. Zhang, S. A. Kulinich, Y. Liu, H. Zeng, *Sci. Rep.* **2014**, *4*, 4976.